HYDROSTATIC PRESSURE MIMICKING DIURNAL SPINAL MOVEMENTS MAINTAINS ANABOLIC TURNOVER IN BOVINE NUCLEUS PULPOSUS CELLS *IN VITRO*

F. Vieira[1], J. Kang[1], L. Ferreira[2] and S. Mizuno[1,*]

[1] Department of Orthopedic Surgery, Brigham and Women's Hospital and Harvard Medical School, Boston, MA 02115, USA
[2] Department of Surgery, Federal University of Sao Paulo, Sao Paulo, Brazil

Abstract

Treatment strategies for progressive intervertebral-disc degeneration often alleviate pain and other symptoms. With the goal of developing strategies to promote the regeneration of the nucleus pulposus (NP), the present study tried to identify the biological effects of hydrostatic (HP) and osmotic pressures on NP cells. The study hypothesis was that a repetitive regimen of cyclic HP followed by constant HP in high-osmolality medium would increase anabolic molecules in NP cells. Bovine NP cells/clusters were enclosed within semi-permeable membrane pouches and incubated under a regimen of cyclic HP for 2 d followed by constant HP for 1 d, repeated 6 times over 18 d. NP cells showed a significantly increased expression of anabolic genes over time: aggrecan, chondroitin sulfate N-acetylgalactosaminyltransferase 1, hyaluronan synthase 2, collagen type 2 ($p < 0.05$). In addition, the expression of catabolic or degenerative genes (matrix metalloproteinase 13, collagen type 1) and cellular characteristic genes (proliferating cell nucleic antigen, E-cadherin) was suppressed. The amount of sulfated glycosaminoglycan increased significantly at day 18 compared to day 3 ($p < 0.01$). Immunostaining revealed deposition of extracellular-matrix molecules and localization of other specific molecules corresponding to their genetic expression. An improved understanding of how cells respond to physicochemical stresses will help to better treat the degenerating disc using either cell- or gene-based therapies as well as other potential matrix-enhancing therapies. Efforts to apply these tissue-engineering and regenerative-medicine strategies will need to consider these important physicochemical stresses that may have a major impact on the survivability of such treatments.

Keywords: Extracellular matrix, nucleus pulposus, hydrostatic pressure, osmotic pressure, metabolic turnover, *in vitro* model.

***Address for correspondence**: Shuichi Mizuno, PhD, Department of Orthopedic Surgery, Brigham and Women's Hospital, 60 Fenwood Road, Boston, MA 02115, USA.
Telephone number: +1 6177326335 Email: smizuno@bwh.harvard.edu

List of Abbreviations

ACAN	aggrecan
ANOVA	analysis of variance
bNP	bovine nucleus pulposus
CDH2	N-cadherin
coHP	constant HP
Col-1	collagen type I (protein)
COL1A1	collagen type I
Col-2	collagen type II (protein)
COL2A1	collagen type II
CSGALNACT1	chondroitin sulfate N-acetylgalactosaminyltransferase 1
CTGF	connective tissue growth factor
cyHP	cyclic HP
DAPI	4,6'-diamidino-2-phenylindole
DMEM	Dulbecco's modified Eagle medium
D-PBS	Dulbecco's phosphate-buffered saline
ECM	extracellular matrix
GAPDH	glyceraldehyde 3-phosphate dehydrogenase
HAS2	hyaluronan synthase 2
HOsm	high osmolality
HP	hydrostatic pressure
HPLC	high-performance liquid chromatography
ITGAV	integrin V

IVD	intervertebral disc
KS	keratan sulfate
LOsm	low osmolality
MMP13	matrix metalloprotein 13
NP	nucleus pulposus
OP	osmotic pressure
PCNA	proliferating cell nuclear antigen
RQ	relative quantity
RT-PCR	reverse transcription polymerase chain reaction
SD	standard deviation
sGAG	sulfated glycosaminoglycan
TRPV4	transient receptor potential cation channel subfamily V member 4

Introduction

IVD degeneration is irreversible (because of the low cellularity and avascularity of the NP tissue) and manifests clinically as chronic pain in the neck and lower back (Alvin *et al.*, 2014). Current first-line treatments are targeted to manage pain, *e.g.*, analgesics and physiotherapy. Patients with late-stage disease and pain refractory to medication are treated surgically by discectomy, spinal fusion, or total disc replacement (Makhni *et al.*, 2016; Snider *et al.*,1999). However, these interventions cannot restore normal biomechanical disc function and instead accelerate degenerative changes within adjacent IVDs (Alentado *et al.*, 2016; Senteler *et al.*, 2017). Therefore, regenerative therapies with the potential to restore spinal function and to offer relief from back pain are of great interest (Sakai and Schol, 2017; Smith *et al.*, 2018; Thorpe *et al.*, 2016). The latest concept for cell-based therapy is to implant therapeutic cells, which then produce a typical NP ECM into the space left after removal of a degenerated NP, ultimately promoting regeneration of the NP tissue (Detiger *et al.*, 2016; Rosenzweig *et al.*, 2018). An important element of this strategy is that the implanted therapeutic cells and resident cells are exposed to dynamic compressive stresses: HP, deviatoric stress, and intradiscal pressure (Sato *et al.*, 1999; Takeoka *et al.*, 2020; Wilke *et al.*, 1999).

Since the NP consists substantially of a fluid, NP cells are exposed to high HP due to diurnal spinal loading. Several studies investigating the effects of HP on NP cells have been conducted using custom-made pressure culture systems (Zvicer and Obradovic, 2018). Most of these studies have demonstrated that HP stimulates anabolic gene expression or production of a typical ECM by NP. However, few studies have addressed innovative therapeutic strategies for IVD regeneration (Le Maitre *et al.*, 2008; Le Maitre 2009; Shah and Chahine 2018). Investigations of the effects of changes in physicochemical stresses on cellular behavior and metabolic turnover require repetitive stress regimens and longer study duration with multiple biomarkers (Mizuno *et al.*, 2019). In addition, a unique characteristic of the NP tissue is the accumulation of sGAG, which generates higher intratissue OP compared to other tissues (Wuertz *et al.*, 2007). Furthermore, NP cells are exposed to intratissue fluid movement by compressive loading, which causes the NP to exude fluid (Ayotte *et al.*, 2001; Vergroesen *et al.*, 2014), and by off-loading, which makes the NP absorb fluid (Vergroesen *et al.*, 2016), resulting in swelling (Neidlinger-Wilke *et al.*, 2012). Thus, to develop regenerative therapies for IVD degeneration, it is important to understand the cellular behavior and metabolic turnover in NPs under diurnal spinal loading (Chan *et al.*, 2011; Haschtmann *et al.*, 2006; Tyrrell *et al.*, 1985).

The metabolic turnover in bNP cells/clusters in response to changes in HP and osmolality was recently evaluated in 12 systematic combinations (Mizuno *et al.*, 2019). bNP cells showed upregulation of anabolic molecules, forming ECM in response to changes in cyHP and in HOsm culture medium (450 mmol/kg H_2O). However, newly accumulated ECM showed gaps (void spaces) under high osmolality but appeared denser under LOsm (320 mmol/kg H_2O) conditions. Since the upregulation of anabolic molecules is usually associated with a dense accumulation of ECM, these results were contradictory. However, Takeoka *et al.* (2020) found that a regimen of cyHP in HOsm followed by coHP in HOsm prevents formation of gaps in the ECM. To further explain these results, the anabolic turnover in NP cells was reproduced under repetitive regimens of changes in HP over multiple days, mimicking the circadian rhythm of spinal loading (Sato *et al.*, 1999; Wilke *et al.*, 1999). The study hypothesis was that a repetitive regimen of cyHP followed by coHP in HOsm medium would reproduce the NP anabolic turnover. To test this hypothesis, primary bNP cells/clusters were seeded within semipermeable membrane pouches and incubated under a repetitive regimen of cyHP at sinusoidal 0.2-0.7 MPa, 0.5 Hz followed by coHP at 0.3 MPa in HOsm for 18 d. The aim was for the cyHP to mimic active upright loading and the coHP to recapitulate intradiscal pressure in the recumbent position. The regenerative (defined as anabolic turnover) and degenerative (defined as catabolic turnover) capabilities of NP cells were evaluated through gene expression analysis and immunohistology of relevant molecules.

Materials and Methods

Isolation of NP cells/clusters

Bovine tails (from 1- to 2-year-old cow) were purchased from a local United States of Department of Agriculture-certified slaughterhouse. Caudal NPs with the adequate margin from the annulus fibrosus were harvested from IVDs using surgical blades (#15 and #22, Bard-Parkers, Aspen Surgical, Caledonia, MI, USA). If any extra fragment of annulus fibrosus remained attached to the NP, it was carefully removed

using scissors. The technique for harvesting the NP was validated histologically and standardized (Fig. 1**a**). The harvested NPs were digested in sterilized 0.15 % collagenase (CLS-1, Worthington Biochemical, Lakewood, NJ, USA) dissolved in Ham's F12 medium (Life Technologies) at 37 °C overnight on a rotator at 8 cycles/min. Usually, 5 NP tissue samples were harvested from one tail and digested in 14 mL of collagenase using a 15 mL conical tube (Falcon®). A minimal volume of air within the conical tube allowed gentle agitation. Then, the NP cells/clusters were rinsed in D-PBS (Life Technologies) twice, seeded onto 1.5 % agarose (1.0 mL, cell culture grade, Sigma-Aldrich)-coated 6-well plates (Falcon®), and incubated for 48 h at 37 °C and 5 % CO_2 in 8 mL of DMEM/Ham's F-12 (1 : 1) supplemented with 10 % fetal bovine serum, 100 U/mL penicillin, and 100 µg/mL streptomycin (Life Technologies). The NP cells/clusters from one tail were seeded onto 3 wells of a 6-well plate. During incubation, the suspended NP cells/clusters aggregated or connected to each other (these connected and aggregated cell, as seen in the digested tissue, were designated as "cell clusters") and the non-digested debris or erythrocytes (if any) settled down on the agarose. This method also allowed for cell clusters in the NP tissue to remain in culture. After 24 h incubation, debris (non-digested matrices) were removed piece by piece using a 200 µL pipette under a dissection microscope. After 48 h incubation, NP cells and cell clusters were collected and rinsed in D-PBS by centrifugation at 95 ×*g* for 5 min, twice.

Preparation of semipermeable membrane pouches and cell seeding

The number of cells in suspended NP cells/clusters collected at 48 h was determined based on DNA concentration, since the NP cells/clusters were often aggregated and could not be separated into individual cells for cell count. The amount of DNA was measured using a fluorescent dye (Hoechst 33258, Molecular Probe) and a fluorometer (TBS-380, Turner Biosystems, Sunnyvale, CA, USA) (Kim *et al.*, 1988). Calf thymus DNA (Sigma-Aldrich) was used as the DNA standard. The correlation between the amount of DNA and the number of cells was validated in independent experiments using bovine NP cells and given 1×10^5 cells as 195 ± 35 ng (mean ± SD, $n = 4$).

Prior to cell seeding, a semipermeable hollow fiber membrane tubing (polyvinylidene fluoride, 1 mm internal diameter, 1.2 mm outside diameter, and 500 kD cut-off molecular weight, Repligen, Rancho Dominguez, CA, USA) was cut into 35 mm-long

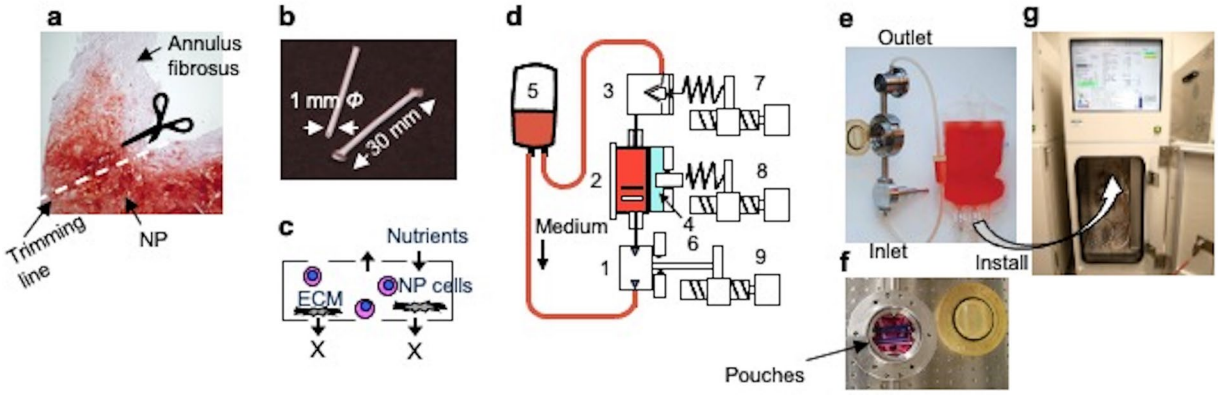

Fig. 1. NP cell/cluster culture using a semipermeable membrane pouch module and HP/perfusion culture system. (**a**) Histological validation of a harvested NP. (**b**) A semipermeable membrane pouch for enclosing NP cells/clusters. The pouch was made of polyvinylidene difluoride (1.0 mm inner diameter, 1.2 mm outer diameter, 30 mm in length, 500 kD MWCO). (**c**) A diagram of the rationale of a semipermeable membrane pouch. Larger molecules *e.g.*, aggrecan, were retained within the pouch, whereas smaller molecules (< 500 kD) in- and out-fluxed through the membrane. (**d**) A diagram of HP/perfusion culture system. The culture system had three components: 1) a pump unit, 2) a pressure culture chamber unit, 3) a backpressure control unit. The culture chamber had a flexible plastic film (tetrafluoroethylene perfluoroalkyl vinyl ether) that separated the culture chamber from 4) the adjacent water compression chamber. Water in the compression chamber was compressed with 8) an actuator-driven piston, and HP was transduced to the medium through the flexible plastic film. HP in the medium and in the water chamber was equivalent so that the pressure within the water compression chamber was monitored using a pressure sensor. Each unit was connected using pressure-proof unions. Outlet of a backpressure control unit and inlet of a medium perfusion pump unit were connected to a medium bag by silicon tubing allowing gas exchange but completely closed to air. 5) Culture medium was kept in a clinically available blood donor bag, hung in an incubator. 6) Culture medium was replenished using a piston pump. 7, 8, 9) Each unit was attached to an actuator in a control system. The maximum magnitude of backpressure was regulated with a spring-attached actuator for constant and cyclic HP. These culture units were completely closed and isolated from the ambient environment. (**e**) HP/perfusion culture module. (**f**) Pouches within a pressure/perfusion culture chamber. (**g**) HP/perfusion culture system.

pieces (Fig. 1**b**,**c**). The pieces were immersed in 100 % ethyl alcohol for 30 min, then autoclaved for 15 min at 121 °C in D-PBS (Mizuno and Ogawa, 2011; Mizuno *et al.*, 2019).

25 μL of the NP cell/cluster suspension (5×10^5 cells/25 μL) was slowly aspirated using a 200 μL tip inserted into the tubing. The tubing was sealed at each end using a stainless-steel clip to form a semipermeable membrane pouch (Fig. 1**a**,**b**). Actual volume of the seeded cell suspension was approximately 25 μL, since 2-3 mm margin at each end of the tubing was needed for closure with the stainless-steel clip (1.0 mm in width).

Incubation of NP cells/clusters

The pouches were divided into 6 groups (Fig. 2).

1. LOsm/No HP group, low-osmolality medium at 320 mmol/kg H_2O for 18 d;
2. HOsm/No HP group, high-osmolality medium at 450 mmol/kg H_2O for 18 d;
3. HOsm/HP group, cyHP at 0.2-0.7 MPa, 0.5 Hz for 2 d in HOsm followed by coHP at 0.3 MPa for 1 d in HOsm, repeated 6 times for 18 d;
4. HOsm/cyHP group, cyHP at 0.2-0.7 MPa, 0.5 Hz in HOsm for 18 d;
5. HOsm/coHP group, coHP at 0.3 MPa in HOsm for 18 d;
6. H-LOsm/HP group: cyHP at 0.2-0.7 MPa, 0.5 Hz in HOsm for 2 d followed by coHP at 0.3 MPa in LOsm for 1 d, repeated 6 times for 18 d.

The pouches were placed in a pressure chamber (Fig. 1**e**,**f**), which was installed in a pressure/perfusion culture system (TEP-2, PURPOSE, Shizuoka, Japan, Fig. 1**g**), to which cyclic or constant HP was applied, with medium replenishment at 0.1 mL/min, 3 % O_2 and 5 % CO_2, mimicking diurnal HP loading in NPs. Briefly, the culture chamber has a backpressure valve/regulator, which precisely regulates backpressure and outlet medium flow (Fig. 1**d**). At the set maximum HP, the amount of replenished culture medium can be ejected precisely. A piston pump can send culture medium into the culture chamber and simultaneously the backpressure valve releases that precise amount of medium. This piston pump can send pressurized fluid at up to 5.0 MPa. The mechanism of this pressurized fluid control is the same as that of an HPLC. For the experimental groups without HP, the pouches were placed in a stainless-steel mesh basket held in 100 mL medium with a stirrer at 5 spins/s to maintain sufficient mass transfer through the semipermeable membrane.

The culture medium at HOsm was prepared with supplemented NaCl at 4.6 g/mL for 450 mmol/kg H_2O. The osmolality of the medium was measured using

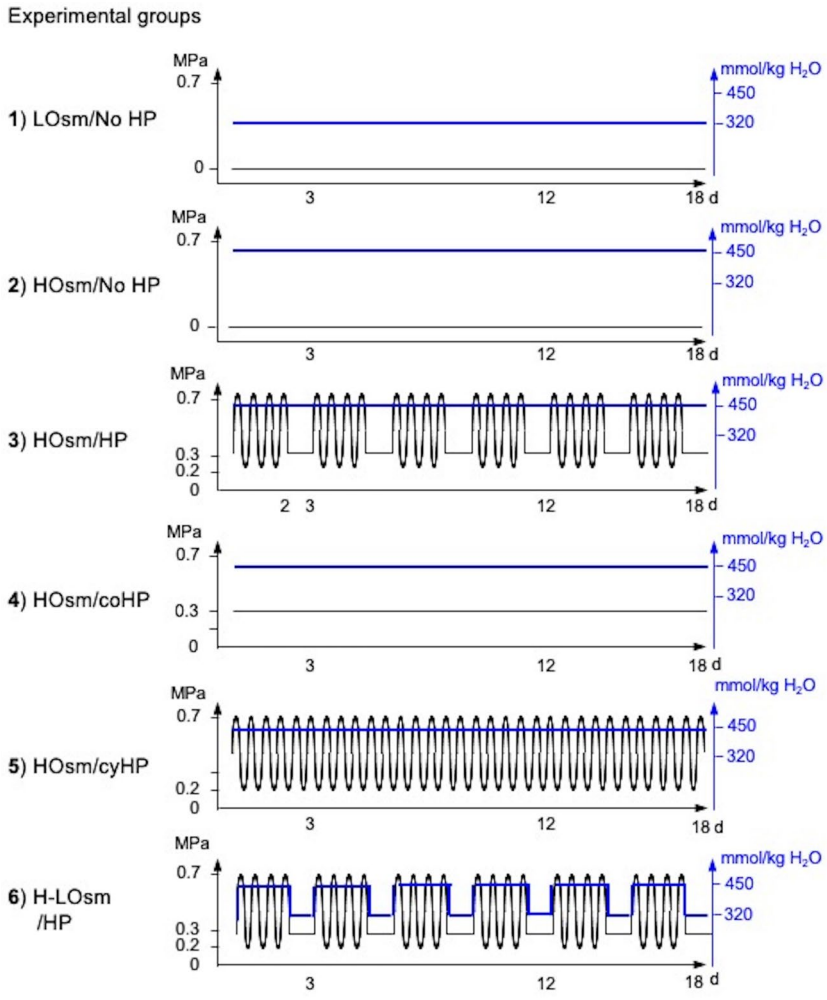

Fig. 2. Systematic culture conditions to compare changes in HP and OP. HP: cyHP at 0.2-0.7 MPa, 0.5 Hz for 2 d followed by coHP at 0.3 MPa for 1 d. LOsm/No HP: 320 mmol/kg H_2O. HOsm/No HP: 450 mmol/kg H_2O. H-LOsm: HOsm for 2 d followed by LOsm for 1 d. No HP: atmospheric pressure.

a freeze-point osmometer (OSMET 5004, Precision System, Natick, MA, USA). If the osmolality was not between 448 and 450 mmol/kg H_2O, additional NaCl was added.

Evaluation of gene expression

The pouches were harvested for RNA extraction, immunohistology as well as sGAG and DNA assays at 3, 12, and 18 d. To quantify gene expression, NP cells/clusters were harvested by flushing the pouches with a guanidine-isothiocyanate-based extraction buffer (Buffer RLT, RNeasy kit®, Qiagen) containing 1 % β-mercaptoethanol for lysing cells prior to RNA isolation. NP cells/clusters were homogenized using a hand-held homogenizer pestle (Fisher Scientific). Total RNA was extracted in accordance with the manufacturer's instructions of the RNeasy kit®. The amount of RNA was determined using a spectrophotometer (NanoDrop ND-1000; Thermo Fisher Scientific) and the samples were kept at − 80 °C until RT-PCR was performed. RNA samples were amplified by RT-PCR using a high-capacity cDNA reverse transcription kit (Life Technologies) to synthesize cDNA. This cDNA was mixed with TaqMan™ Gene Expression Master Mix (Life Technologies) and the fluorescent-labeled probe of the desired molecule (TaqMan™ probe, Life Technologies), followed by measuring gene expression by real-time PCR (QuantStudio™, Applied Biosystems). TaqMan gene expression assays were *ACAN*: Bt03212189_m1; *CSGALNACT1*: Bt03272948_m1; *HAS2*: Bt03212694_g1; *COL2A1*: Bt03251837_mH; *COL1A1*: Bt03225358_g1; *CTGF*: Bt03212492_m1; *MMP13*: Bt03214051_m1; *PCNA*: Bt03211154_g1; *CDH2*: Bt04298958_m1; *ITGAV*: Bt04299013_g1; *GAPDH*: Bt03210919_g1 (Life Technologies). Expression Suite Software v.1.0.4 (Thermo Fisher Scientific) was used to convert from ΔCt to RQ.

Measurement of accumulated sGAG and DNA

Newly synthesized sGAG and DNA produced by bNP cells were measured biochemically. The experiments were conducted independently for quantitative evaluation of sGAG and DNA. At days 3, 12, and 18, the pouches were harvested and the sample was ejected from each pouch by replenishing 200 μL of 125 μg/mL papain solution (Sigma-Aldrich) into a 0.5 mL tube with a cap and digested at 60 °C for 18 h. The optical density of sGAG was quantified with dimethylmethylene blue (Farndale *et al.*, 1982) at 570 nm using a microplate reader (iMark™, Bio-Rad). Shark chondroitin sulfate (Sigma-Aldrich) was used for the standard. The same sample was used for DNA assay, as described in the cell seeding section above.

Cell viability

Independent experiments were conducted to determine cell viability. At 18 d, pouches were harvested and samples ejected by injecting D-PBS (Fig 3**a**). One pouch was harvested from each group. Cell viability assays were conducted three times. The samples were minced using double-stacked shaver blades and incubated at room temperature for 30 min in 1 μmol/L calcein AM (to detect live cells) and 2 μmol/L ethidium homodimer-1 (to detect dead cells) diluted in D-PBS using a LIVE/DEAD® Assay kit (Life Technologies) (Papadopoulos *et al.*, 1994). Then, the samples were rinsed 3 times in D-PBS for 10 min and cover-slipped using mounting medium with DAPI (SlowFade™ Gold antifade reagent with DAPI, Invitrogen) and processed for imaging. Live cells were labelled in green (exposure: 450-490 nm; emission: 500-550 nm), dead cells in red (exposure: 540-580 nm; emission: 592-660 nm), and nuclei in blue (exposure: 325-375 nm; emission: 435-485 nm) and visualized using an inverted fluorescence microscope (DMi 8, Leica Microsystem). The images were acquired using a 20× objective lens and a DFC 7000T camera (Leica Microsystems). Since most cells were green (live), red and blue cells (nuclei) were counted manually within the same defined square (150 × 150 pixels) to avoid overcounting live cells due to the thickness of the sample.

Immunohistological evaluation

NP cells/clusters were harvested at days 3, 12, and 18 by flushing them from the pouches using D-PBS. Samples were fixed in a 2 % paraformaldehyde/0.1 mol/L cacodylate buffer (pH 7.4) at 4 °C. Since the samples flushed were fragile and of a round-bar shape, they were immobilized within a 3 % agarose gel (Genetic analysis grade, Fisher Scientific) dissolved in water. These samples were trimmed, embedded in paraffin-wax, and cut into 7 μm-thick sections for immunostaining.

Dewaxed sections were rinsed in PBS and pretreated with 0.3 % hydrogen peroxide for 20 min. For KS immunostaining, the sections were incubated for 30 min at 37 °C in 0.05 units/mL chondroitinase ABC (Sigma-Aldrich) dissolved in Tris-Base buffer (pH 7.4) with proteinase inhibitor cocktail (Roche Complete, Sigma Millipore). For immunohistology with other antibodies, this chondroitinase ABC digestion was omitted. Sections rinsed three times in PBS were blocked using 3 % normal horse serum (Vectastain™ ABC kit, Vector Laboratory) in a humidified chamber for 30 min at room temperature, followed by incubation with a primary antibody against KS (1 : 200, mouse monoclonal antibody 4B3/D10, Santa Cruz Biotechnology). Mouse IgG (Sigma-Aldrich) was used as a negative control. For other immunostaining, the sections were incubated for 30 min at room temperature with a primary antibody: Col-1 (rabbit anti-Col-1, 1 : 300, Abcam), Col-2 (rabbit anti-Col-2, 1 : 200, MyBioSource, San Diego, CA, USA), MMP13 (rabbit anti-rat MMP13, cross-reactivity with bovine MMP13, 1 : 200, LSBio, Seattle, WA, USA), and PCNA (rabbit anti-PCNA, 1 : 200, Abcam). Rabbit normal IgG (Vector Laboratory) was used as a negative control for polyclonal antibodies. Following incubation with the primary antibody, the

sections were rinsed three times in PBS and incubated with a second biotinylated antibody according to the manufacturer's instructions (Universal Vectastain™ ABC kit). Color was developed using 3,3'-diaminobenzidine (DAB kit, Vector Laboratory). Counterstaining was performed using Harris's hematoxylin (Sigma-Aldrich) for KS and Col-2, and Contrast RED (KPL, Laboratories, Gaithersburg, MD, USA) for Col-1, MMP13, and PCNA.

Data analysis of gene expression and biochemistry

The RQ of the expression of each gene was calculated according to the difference between the average of each condition (time of experiment in each group) and of the LOsm/No HP (control) at day 3, which was given a value of 1.0. RQ was analyzed using a one-way ANOVA followed by a Bonferroni test for comparison of all conditions, with $p < 0.05$ considered significantly different (SPSS, version 21; IBM). The experiments were conducted 5 times, using different cow tails each time. After outliers were eliminated with a Shapiro-Wilk test, statistical analyses of 4 or 5 samples were conducted. The concentrations of sGAG and DNA at 3, 12, and 18 d were converted to the amount per pouch. The concentrations of sGAG and DNA at 3, 12, and 18 d were converted to the amount per pouch. The amounts of sGAG and DNA under HOsm and HOsm/HP at each time point, and in each group at 12 and 18 d, were compared to day 3 data using a Student's *t*-test.

Results

Cell viability

Viable cells, with their characteristic sharp peripheries, were easily identified within aggregated clusters and individually in all experimental groups. Red-stained dead cells were rare, and small particles were often seen randomly within and around the aggregation (Fig. 3**b**). The viability of each group was more than 90 %. There was no significant difference between groups (Fig. 3**c**). Although a few dead cells were seen in selected regions of interest using a microscope, retention of these dead cells was unavoidable, because cells/clusters formed a 3D mini-tissue-like structure within a semipermeable membrane pouch (molecular-weight cut-off of 500 kD).

Gene expression in NP cells in response to repetitive regimens of Osm and HP

Anabolic and regenerative turnover

Expression of *ACAN*, *CSGALNACT1*, *HAS2*, and *COL2A1*, genes encoding for anabolic molecules, was

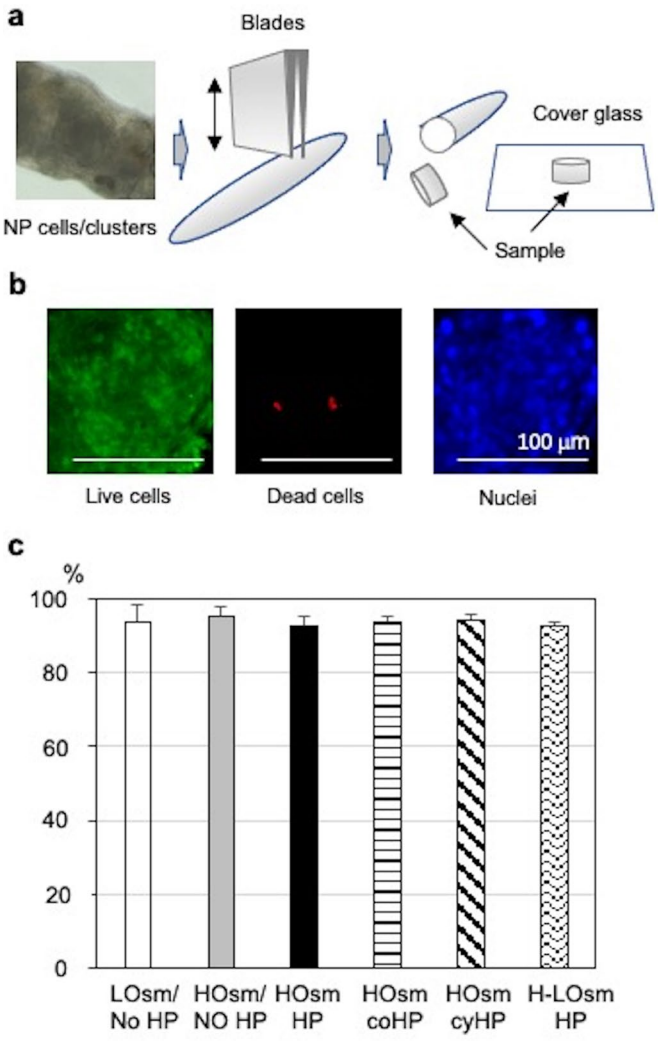

Fig. 3. Cell viability. (**a**) Sample preparation from 3D NP cells/clusters ejected from a pouch, minced, and stained with a fluorescent dye. (**b**) NP cells stained with a fluorescent dye. Live cells in green, dead cells in red, and nuclei in blue. (**c**) Cell viability ($n = 3$).

quantified in NP cells exposed to various regimens of combinations of OP and HP (Fig. 4**a**).

bNP cells maintained steady levels of expression of *ACAN* for 18 d under LOsm/No HP conditions (control). On the other hand, under HOsm/No HP conditions the expression of *ACAN* was transiently upregulated at day 12 and declined at day 18. With HOsm/HP, bNP cells expressed significantly more *ACAN* with time, *i.e.*, 2.6, 4.2, and 5.2 times more than that in LOsm/No HP conditions at days 3, 12, and 18, respectively ($p < 0.01$). After exposure to cyHP and coHP, *ACAN* expression increased significantly: 3 and 3.7 times compared to that in LOsm/No HP at day 12, respectively, and maintained roughly those levels until day 18. In H-LOsm/HP conditions, bNP cells maintained a *ACAN* expression level similar to that at day 3 for 18 d.

bNP cells maintained the expression of *CSGALNACT1* at levels similar to that at day 3 for 18 d in the LOsm/No HP control. On the other hand, *CSGALNACT1* expression increased significantly under HOsm/No HP conditions: 1.7-, 2.6-, and 3.6-fold

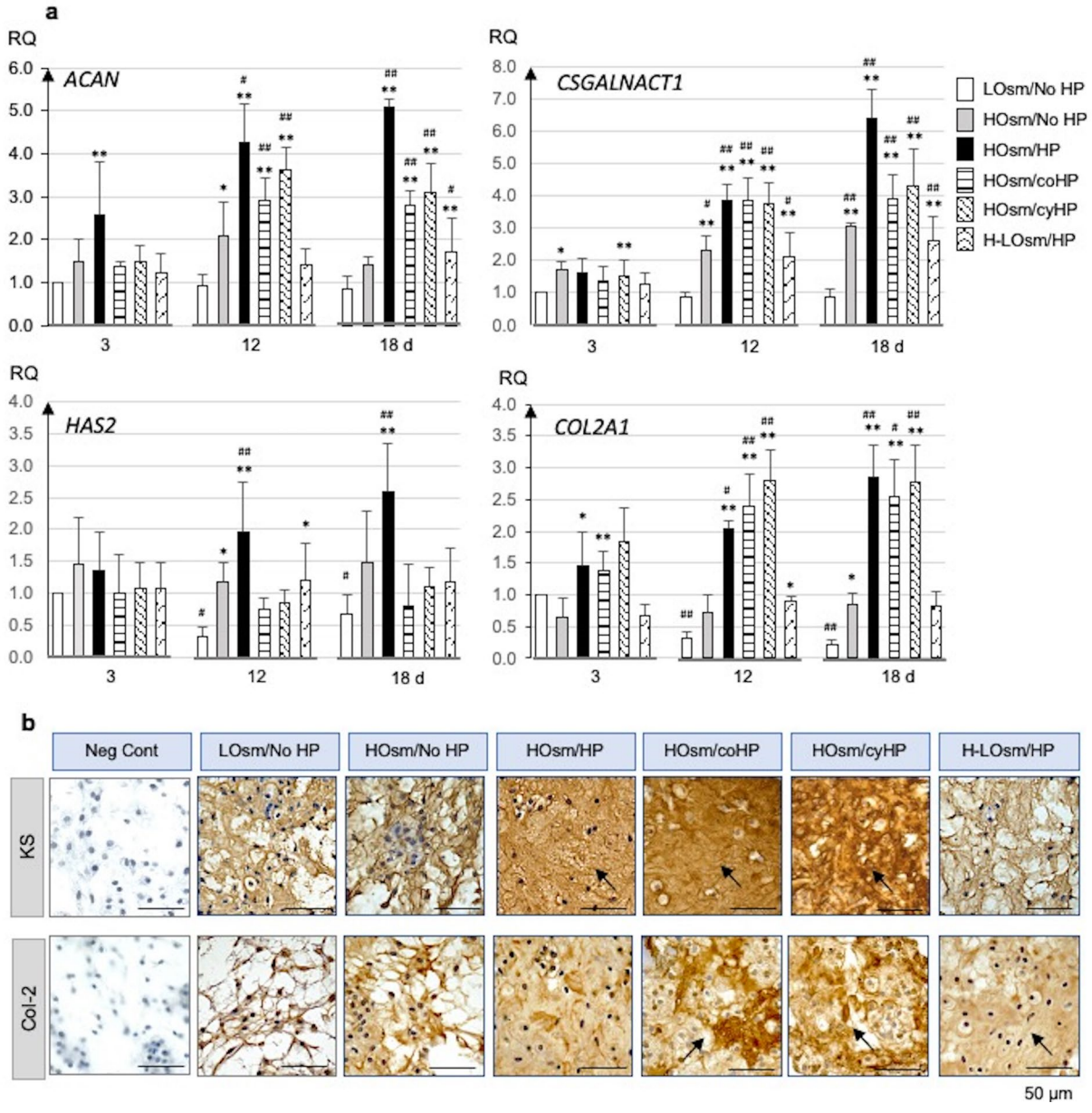

Fig. 4. Gene expression profiles and immunohistology of anabolic molecules by NP cells/clusters in response to repetitive changes in cyclic followed by constant HP in HOsm or LOsm. (**a**) RQ of the expression of *ACAN*, *CSGLUNACT1*, *HAS2* and *COL2A1*. Bars indicate mean ± SD ($n = 5$). Two-way ANOVA was conducted between regimens at the same day (**$p < 0.01$; *$p < 0.05$) and between 12 or 18 d and control at 3 d within each regimen ($^{\#\#}p < 0.01$; $^{\#}p < 0.05$). (**b**) Accumulation of sub-molecule of KS and Col-2 at 18 d. Each molecule accumulated was stained in brown and counterstained with hematoxylin in blue. Arrows indicate intense accumulation of KS and Col-2. Neg Cont: negative control. LOsm: 320 mmol/kg H_2O. HOsm: 450 mmol/kg H_2O. HP: cyHP at 0.2-0.7 MPa, 0.5 Hz for 2 d followed by coHP at 0.3 MPa for 1 d. H-LOsm: HOsm for 2 d followed by LOsm for 1 d. No HP: atmospheric pressure. Each section was 7 µm-thick. Scale bar: 50 µm.

compared with the LOsm/No HP control at days 3, 12, and 18 ($p < 0.05$), respectively. With HOsm/HP, bNP cells expressed significantly more *CSGALNACT1*: 2.1-, 2.4-, and 1.5-fold more than in the LOsm/No HP control at days 3, 12, and 18, respectively ($p < 0.05$). Under cyHP and coHP conditions, *CSGALNACT1* showed a similar upregulation: 3.9 and 3.7 times that in the LOsm/No HP control at day 12, respectively, and maintained those levels until day 18. In H-LOsm/HP conditions, bNP cells showed a significant increase in *CSGALNACT1*: 1.8 and 2 times that in LOsm/No HP control at days 12 and 18, respectively ($p < 0.05$).

In the LOsm/No HP control, expression of *HAS2* decreased with time. However, under HOsm/HP conditions, *HAS2* expression was significantly higher (1.9 and 2.6 times) compared to LOsm/No HP control at days 12 and 18, respectively ($p < 0.05$). With other regimens, *HAS2* maintained levels similar to those seen at day 3 for 18 d.

In LOsm/No HP control, bNP cells had a decreased expression of *COL2A1* with time. However, under HOsm/No HP conditions, the expression of *COL2A1* was maintained at day 3 levels for 18 d. Under HOsm/HP, cyHP, and coHP conditions, *COL2A1* expression was increased 1.5, 2.0, and 2.9 times compared with LOsm/No HP levels at day 3, respectively ($p < 0.05$), and maintained similar levels until day 18. Under H-LOsm/HP, *COL2A1* maintained levels similar to those seen on day 3 for 18 d.

Catabolic/degenerative turnover

The expression of *COL1A1* and *MMP13*, genes encoding for the production of catabolic molecules (Fig. 5**a**), was quantified. In bNP cells, expression of *COL1A1* was significantly increased in LOsm/No HP control with time ($p < 0.01$). Under HOsm, HOsm/HP, and H-LOsm/HP conditions, *COL1A1* maintained levels similar to those at day 3 for 18 d. After exposure to cyHP and coHP, *COL1A1* showed a transient increase at day 12.

MMP13 was significantly increased in bNP cells, 2.0 and 4.8 times more at days 12 and 18 ($p < 0.01$), respectively, than that in the LOsm/No HP control at day 3 (Fig. 5**a**). With other regimens, *MMP13* was downregulated compared to LOsm/No HP at day 3 and maintained that level for 18 d.

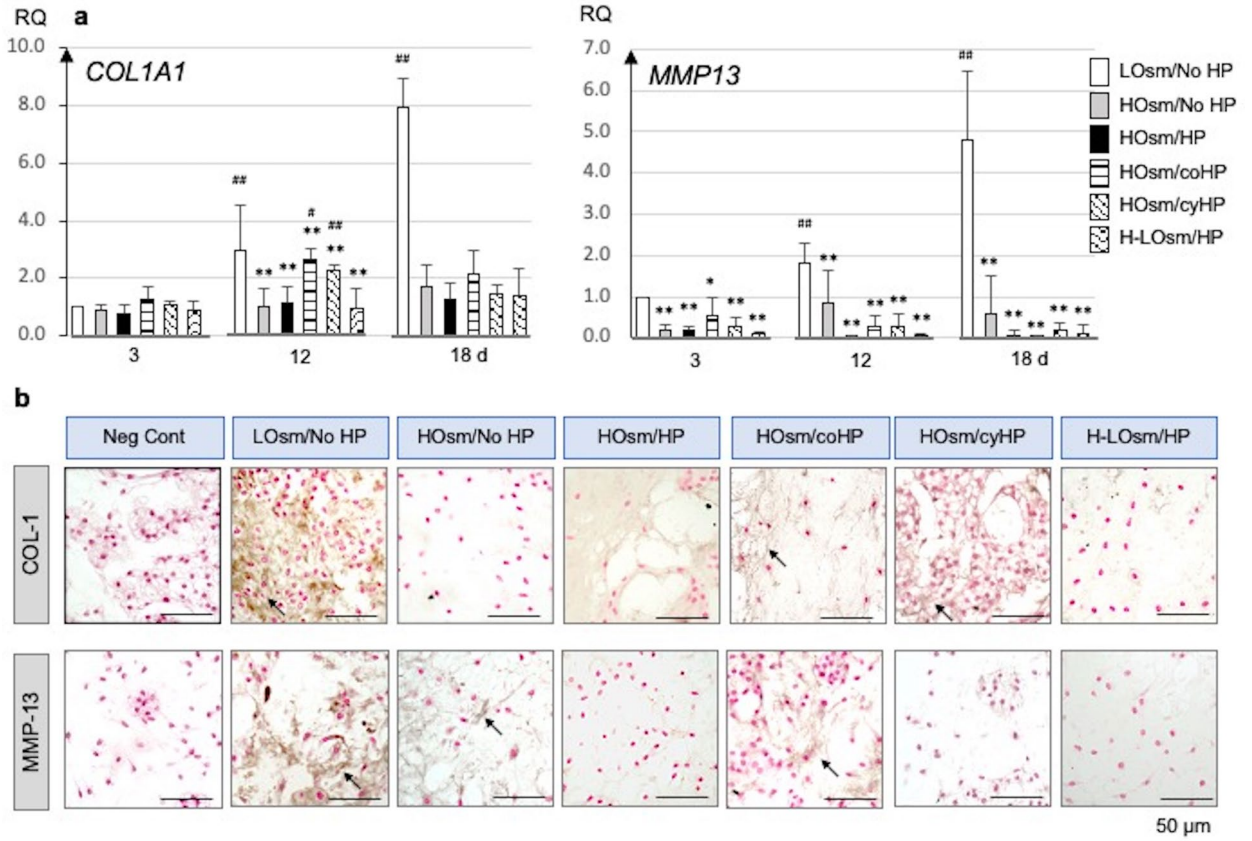

Fig. 5. Gene expression profiles and immunohistology of catabolic molecules by NP cells/clusters in response to repetitive changes in cyclic followed by constant HP in HOsm or LOsm. (**a**) RQ of the expression of *MMP13* and *COL1A1*. Bars indicate mean ± SD ($n = 5$). Two-way ANOVA was conducted between regimens at the same day (**$p < 0.01$; *$p < 0.05$) and between 12 or 18 d and control at 3 d within each regimen ($^{\#\#}p < 0.01$; $^{\#}p < 0.05$). (**b**) Accumulation of Col-1 and MMP13 at 18 d. Each molecule was stained in black and counterstained in red. Arrows indicate intense accumulation of each molecule. Neg Cont: negative control. LOsm: 320 mmol/kg H_2O. HOsm: 450 mmol/kg H_2O. HP: cyHP at 0.2-0.7 MPa, 0.5 Hz for 2 d followed by coHP at 0.3 MPa for 1 d. H-LOsm: HOsm for 2 d followed by LOsm for 1 d. No HP: atmospheric pressure. Each section was 7 µm-thick. Scale bar: 50 µm.

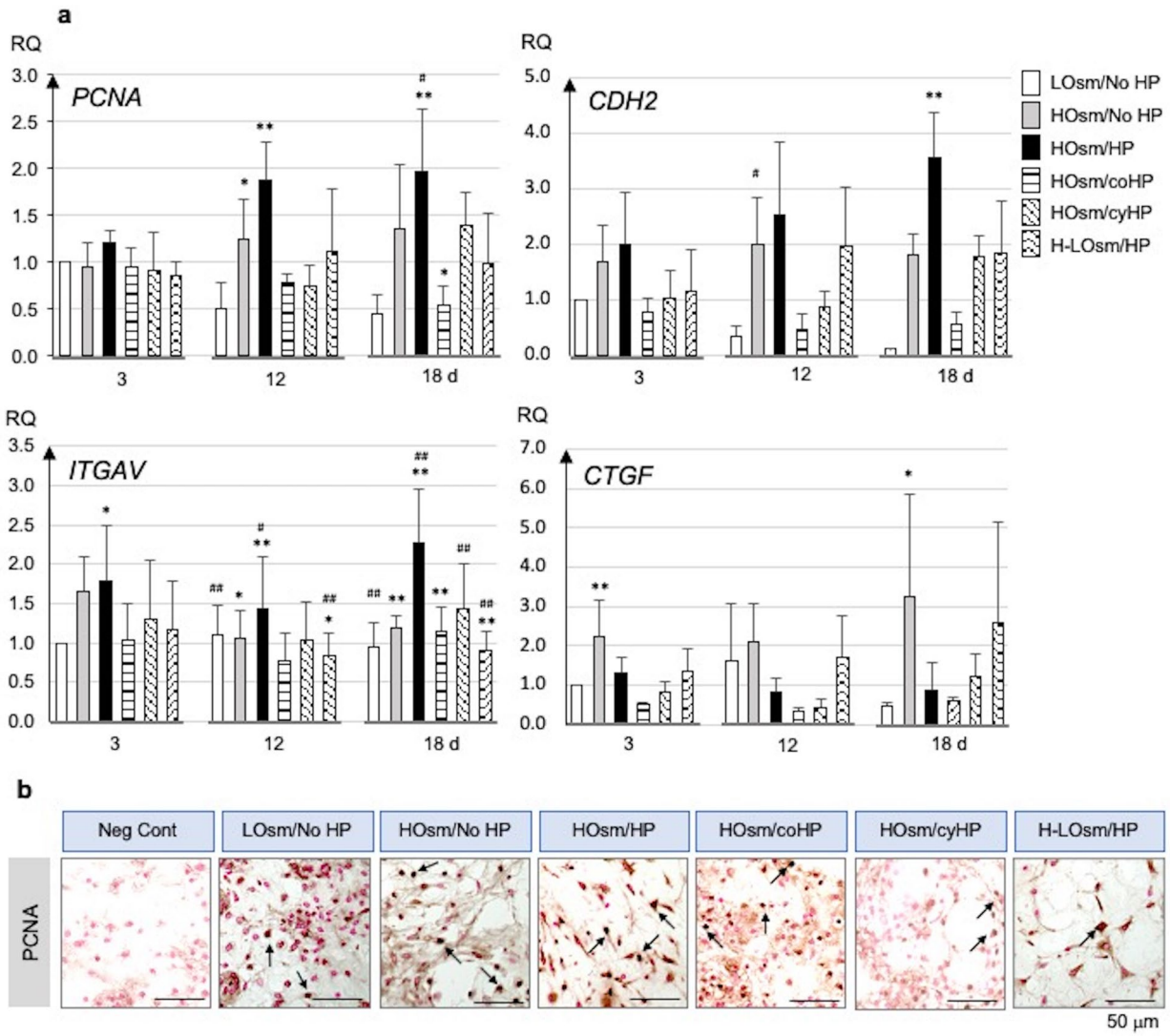

Fig. 6. Gene expression profiles and immunohistology of cellular characteristic molecules (proliferation and adhesion) by NP cells/clusters in response to repetitive changes in cyclic followed by constant HP in HOsm or LOsm. (**a**) RQ of the expression of *PCNA*, *CDH2*, *ITGAV*, and *CTGF*. Bars indicate mean ± SD (n = 5). Two-way ANOVA was conducted between regimens at the same day (**p < 0.01; *p < 0.05) and between 12 or 18 d and control at 3 d within each regimen ($^{\#\#}p$ < 0.01; $^{\#}p$ < 0.05). (**b**) Proliferating cells (PCNA) are stained in black and counterstained in red. Arrows indicate examples of PCNA positive cells. Neg Cont: negative control. LOsm: 320 mmol/kg H_2O. HOsm: 450 mmol/kg H_2O. HP: cyHP at 0.2-0.7 MPa, 0.5 Hz for 2 d followed by coHP at 0.3 MPa for 1 d. H-LOsm: HOsm for 2 d followed by LOsm for 1 d. No HP: atmospheric pressure. Each section was 7 µm-thick. Scale bar: 50 µm.

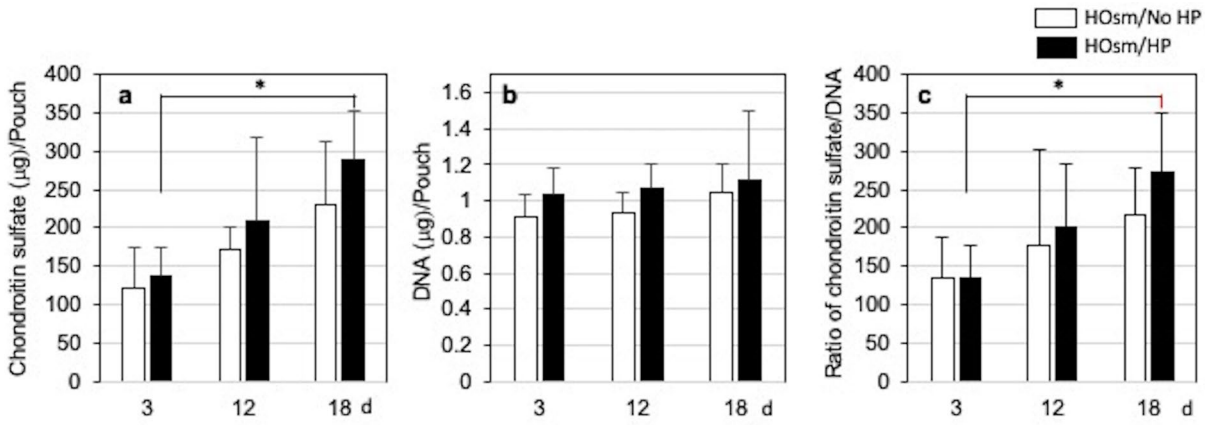

Fig. 7. Amounts of accumulated sGAG and DNA produced by bNP cells/clusters under HOsm/No HP and HOsm/HP over 18 d. (**a**) Amount of sGAG produced by NP cells/clusters. (**b**) Amount of DNA. (**c**) Ratio of sGAG/DNA. Bars indicate mean ± SD (n = 5).

Cellular characteristic markers (cell proliferation, adhesion, phenotypes)

The expression of *PCNA*, *ITGAV*, and *CDH2*, genes encoding for the production of cellular characteristic molecules, was quantified (Fig. 6**a**). Under LOsm/No HP conditions (control), expression of *PCNA* was reduced considerably (50 %) at days 12 and 18. Under HOsm/HP conditions, *PCNA* expression was significantly increased: 3.7 and 4.3 times more compared to that in the LOsm/No HP control at days 12 and 18, respectively ($p < 0.05$). Under cyHP, H-LOsm/HP and HOsm/No HP, *PCNA* maintained day 3 expression levels for 18 d (Fig. 6**a**).

Under HOsm/HP conditions, the expression of *ITGAV* was significantly upregulated at day 18; however, with other regimens, it maintained day 3 expression levels for 18 d (Fig. 6**a**).

Under LOsm/No HP (control) and cyHP, expression of *CDH2* decreased of 20 % and 50 %, respectively, at day 18 compared to day 3 LOsm/No HP. Under HOsm/No HP conditions, expression of *CDH2* was upregulated at day 3 compared to that under LOsm/No HP and maintained that level for 18 d. Under HOsm/HP, *CDH2* was significantly increased with time when compared to its expression in the LOsm/No HP control at day 3 ($p < 0.05$). Under coHP, *CDH2* doubled its expression at day 18, compared to day 3. Under H-LOsm/HP, *CDH2* expression was 2-fold higher at day 12 compared to day 3 and remained at the same level at day 18 (Fig. 6**a**).

bNP cells showed a trend of increasing *CTGF* under HOsm/No HP and H-LOsm/HP conditions for 18 d. However, with other regimens, the expression of *CTGF* showed a trend towards downregulation or maintained day 3 levels for 18 d (Fig. 6**a**).

Immunohistology

Gene expression was characterized immunohistologically by evaluating the quality of accumulated ECM, the localization of degenerative enzymes, and cell proliferation.

Immunohistology was used to evaluate the presence of KS on aggrecan, a typical component of cartilage ECM, surrounding NP cells (Fig. 4**b**). In the absence of HP, there appeared to be homogeneous distribution of KS associated with large gaps. However, under HOsm/HP denser accumulation of KS occurred with time. The distinct difference was that a dense area of ECM free of gaps was seen under HOsm/HP at day 18.

Immunolabelling for Col-2 was performed to evaluate the quality of a typical NP cartilage ECM (Fig. 4**b**). Under HOsm/No HP, low levels of Col-2 accumulation and the presence of gaps were observed at day 18. Under HOsm/HP, there was a considerably more intense Col-2 accumulation and homogeneity in NP clusters with time.

Immunolabelling using anti-Col-1 was performed to identify a fibrous ECM (Fig. 5**b**). Under LOsm conditions, the amount of Col-1 appeared to increase in intensity with time. Under HOsm/No HP conditions for 18 d, Col-1 accumulated within NP clusters. However, Col-1 intensity faded under HOsm/HP and H-LOsm/HP over 18 d.

Immunolabelling for MMP13 was performed to assess ECM degeneration (Fig. 5**b**). In the LOsm/No HP group, there was an intense MMP13 labelling in the ECM of NP cells/clusters at day 18. Under HOsm/No HP conditions, labelling for MMP13 was slight around cells. With other regimens, there was no detectable MMP13 within NP clusters.

Immunolabelling using anti-PCNA was performed to identify proliferating cells and to semi-quantitatively evaluate the number of these cells (Fig. 6**b**). PCNA-positive cells were common within the NP cells/clusters under all regimens and were more abundant under HOsm/No HP, HOsm/HP, and H-LOsm/HP than LOsm/No HP.

Accumulation of sGAG and DNA

Accumulated sGAG and DNA were measured (Fig. 7). Compared to day 3, the amount of sGAG produced by NP cells/clusters under HOsm/HP increased 2.1-fold (statistically significant) by day 18 ($p < 0.01$). Under HOsm/No HP, the amount of sGAG appeared to increase between days 3 and 18, but the results were not statistically significant. The amount of DNA in each group remained steady over 18 d of culture. There was no statistical significant difference between the effects of HOsm and HOsm/HP. The sGAG/DNA ratio detected in NP cells/clusters under HOsm/HP conditions increased significantly (1.9-fold) by day 18 when compared to day 3 ($p < 0.01$).

Discussion

The aim of the present study was to elicit anabolic turnover in primary bNP cells under alternating HP modes in HOsm medium *in vitro*. The study hypothesis was that mimicking diurnal spinal loading on NP cells, by alternating cyHP and coHP in HOsm medium, would stimulate anabolic turnover in bNP cells. To elucidate the effects of these stresses on anabolic turnover, LOsm (control, medium osmolality 320 mmol/kg H_2O), HOsm (no HP control, medium osmolality 450 mmol/kg H_2O), HOsm/cyHP (continuous cyHP at 0.2-0.7 MPa, 0.5 Hz), HOsm/coHP (continuous coHP at 0.3 MPa), repetitive HOsm/HP (alternating HP modes: cyHP for 2 d followed by coHP for 1 d), and repetitive H-LOsm/HP (HOsm/cyHP-LOsm/coHP) were compared (Fig. 2).

Rationale for HOsm comparison to LOsm

bNP cells/clusters show upregulated gene expression of ECM molecules in HOsm conditions at day 7 (Mizuno *et al.*, 2019). Therefore, HOsm group was assumed to mimic conditions similar to those in normal NP tissue, where HOsm is higher than OP in physiological fluid (320 mmol/kg H_2O). However, because this OP in intra-NP tissue (defined as ECM-

associated OP) was the estimated value converted from the fixed charged density (Wuertz *et al.*, 2007), it was unclear whether the osmolality in the culture medium was equivalent to that within the ECM around each cell (Neidlinger-Wilke *et al.*, 2014). Enzymatically isolated NP cells/clusters were used that were consistently exposed to HOsm in culture medium. It is believable that HOsm interacted directly with bNP cells because of the negligible accumulation of ECM at the start of culture. However, newly synthesized ECM accumulated around cells with time. At later time points, the effects of HOsm may be replaced by ECM-associated OP or synergistically increased with ECM. Under LOsm conditions, *COL1A1* and *MMP13* were significantly upregulated compared to HOsm conditions with/without HP. HOsm and/or ECM-associated OP can inhibit synthesis of fibrotic ECM and enzymatic degeneration. The comparison of HOsm with LOsm *in vitro* addressed the possibility that degenerated NP with annulus fibrosus injury (loss of intradiscal pressure) or loss of ECM increased the risk of progressive degeneration. To maintain anabolic turnover and support the regeneration of NP, a highly osmotic environment would be necessary.

Rationale behind the regimen of combined HOsm and HP

Mizuno *et al.* (2019) demonstrated that a 7 μm-thick section shows gaps (non-stained empty spaces) within the accumulated ECM synthesized by bNP cells under HOsm conditions. On the other hand, such gaps were absent from the LOsm/No HP control sample. If these gaps were created due to ECM degeneration, there would be less upregulation of anabolic and/or catabolic genes' expression. Another possible cause was weak entanglement of ECM due to excessive absorption of fluid by the ECM associated with high OP. Although these gaps may be unavoidable when forming amorphous NP tissue, the present study sought to identify a specific regimen of physicochemical stresses to prevent the formation of these gaps. In normal IVDs, the NP is compartmentalized within the IVD segment, which always maintains the intradiscal pressure. Thus, this intradiscal pressure was mimicked using coHP. More recently, Takeoka *et al.* (2020) have demonstrated that cyHP followed by coHP prevents the formation of gaps in the ECM formed by the bNP cells over 6 d. To assess the consequences of coHP for metabolic turnover in NP cells, the effects of i) a repetitive regimen of cyHP at 0.2-0.7 MPa, 0.5 Hz, ii) HOsm for 2 d followed by coHP at 0.3 MPa, iii) HOsm for 1 d over 18 d were compared with other chosen regimens. Since coHP loading prevented formation of ECM gaps, intradiscal pressure should be maintained for NP regeneration.

Rationale for HP magnitude and mode

Several studies investigating the effects of pure HP or compressive stresses on metabolic turnover in NP cells have been conducted using monolayered NP cell culture, three-dimensional cell culture in gel (*e.g.*, alginate, Neidlinger-Wilke *et al.*, 2014), NP explants, organ culture (Emanuel *et al.*, 2015; Gantenbein *et al.*, 2006), and animal models (Alini *et al.*, 2008). Through various positions and types of spinal motion, native NP tissues are under compressive stresses, which include pure HP and pure deviatoric (distortional or shear) stress (Carter and Beaupre, 2001). Since normal NP tissue is abundantly hydrated, it is reasonable to assume that the stress was primarily pure HP in NP tissue (Urban and McMullin, 1988), with accompanying intradiscal pressure in IVD (Sato *et al.*, 1999; Walter *et al.*, 2011; Wilke *et al.*, 1999). Thus, the present study intended to recapitulate the effects of pure HP in NP cells within an amorphous hydrated tissue compartment.

bNP cells isolated from bovine tails were chosen because the physicochemical properties seen in human IVD are similar in several aspects to those of bovine tails. The range of motion of the human lumbar spine is similar to that of the bovine tail (Alini *et al.*, 2008; Demers *et al.*, 2004). Furthermore, the swelling pressure of the NP in bovine tails is similar to that found in the human lumbar IVD, estimated at 0.25 MPa, which was converted from the height of the vertebrae (Oshima *et al.*, 1993). Intradiscal pressure in human lumbar discs in prone and recumbent positions is estimated at 0.1-0.3 MPa (Wilke *et al.*, 1999), which can be defined as coHP. In addition, dynamic spinal motion is critical to maintain metabolic turnover in avascular IVD (Neidlinger-Wilke *et al.*, 2014). Magnitude and mode of HP vary depending on spinal position and physical activity (Gantenbein *et al.*, 2006; Neidlinger-Wilke *et al.*, 2014). Dynamic magnitudes have been estimated to range from 0.2 to over 3 MPa, and constant magnitude would be around 0.2 MPa regardless of posture or activity (Alini *et al.*, 2008; Sato *et al.*, 1999). Occasionally, the IVD is subjected to a higher-magnitude HP (> 3 MPa), which leads to degeneration of IVD cells, mediating increases in MMPs and decreasing ECM synthesis (Alini *et al.*, 2008; Kasra *et al.*, 2006). When NP cells were incubated under physiological HP ranging between 0.3 and 1 MPa, ECM proteoglycan synthesis was upregulated, while other conditions cause a downregulation in ECM and upregulation of catabolic signaling (Handa *et al.*, 1997; Hutton *et al.*, 1999; Hutton *et al.*, 2001; Ishihara *et al.*, 1996; Le Maitre *et al.*, 2008; Mizuno *et al.*, 2019). Based upon the above physiological magnitude and mode of HP, the *in vitro* regimen of HP loading was established to recapitulate the anabolic turnover. Although this regimen was designed for the present *in vitro* study, it was very close to what occurs naturally in human spinal loading. This may be a considerable advantage for the dynamic translational model of the human IVD.

Rationale for duration of HP loading

The durations of one regimen of HP and total duration of repetitive regimens of HP were varied for research purposes (Gantenbein *et al.*, 2006). For example,

Table. 1. Effects of changes in physicochemical stresses on metabolic turnover in bovine normal NP tissue models (cells/clusters) over 18 d (5 repetitions).

	Regenerative/anabolic				Degenerative/ catabolic		Phenotype/behavior			
Condition	*ACAN*	*CSGALN-ACT1*	*HAS2*	*COL2A1*	*COL1A1*	*MMP13*	*CTGF*	*PCNA*	*ITGA5*	*CDH2*
LOsm/No HP	→	→	↓	↓↓	↑↑	↑↑	↓	↓	→	↓↓
HOsm/No HP	↑	↑↑	↑	→	→	→	↑↑	→	→	↑
HOsm/HP	↑↑↑	↑↑↑	↑↑	↑↑↑	→	↓↓	→	↑	↑↑	↑↑
HOsm/coHP	↑↑	↑↑	→	↑↑↑	→	↓↓	→	↓	→	→
HOsm/cyHP	↑↑	↑↑	→	↑↑↑	→	↓↓	→	→	→	→
H-LOsm/HP	↑	↑↑	→	→	→	↓↓	↑↑	↓	→	→

→ Nearly constant ↓ Slight decrease ↓↓ Moderate/large decrease

↑ Small increase ↑↑ Moderate increase ↑↑↑ Large increase

some researchers applied HP for a few hours per day followed by no HP for the rest of the day, repeated each day for several days (Gantenbein *et al.*, 2006; Kasra *et al.*, 2006). In previous *in vitro* studies, HP loading was set for 3 d in order to determine possible differences in gene expression between the no-HP control and the HP-loading group (Mizuno *et al.*, 2019; Mizuno and Ogawa, 2011; Ogura *et al.*, 2019). Repetitive regimens were also included to explore the effects of accumulated ECM on isolated NP cells/clusters over time. Thus, repetitive regimens were created that cycled 6 times over 18 d and evaluated quantitative gene expression, accumulation of ECM, and immunohistology at 3 time points over 18 d. Gene expression profiles showed an increasing trend from 3 to 18 d, and a plateau at either 3-18 d or 12-18 d. The increased *ACAN* under HOsm/HP was possibly stimulated with newly accumulated ECM as positive feedback over 18 d. In addition, gene expression of *COL1A1* under HOsm/No HP plateaued, whereas it was significantly upregulated under LOsm/No HP. Thus, *COL1A1* expression was sensitive to osmolality. Furthermore, *MMP13* was suppressed under any regimen involving HP over 18 d. Overall, regimens repeated 6 times over 18 d recapitulated altering metabolic balances. By manipulating these regimens and duration, the NP cell/cluster model has the potential to reproduce homeostasis and regenerative process in NP tissue.

Effects of repetitive regimen of HOsm/HP on metabolic turnover and cellular characteristics in NP cells

The effects of physicochemical stresses were categorized into regenerative/anabolic turnover, degenerative/catabolic turnover, and cellular characteristics (Fig. 4-6, Table 1).

Regenerative/anabolic turnover

Under repetitive HOsm/HP, genes for several important constituents of aggrecan were upregulated: *ACAN*, an aggrecan core-protein that binds chondroitin sulfate and KS chains to form large proteoglycans (Hascall and Heinegard, 1974); *CSGALNACT1*, an enzyme that transfers chondroitin sulfate N-acetylglucosamine to elongate chondroitin sulfate chains (Ishimaru *et al.*, 2014; Sakai *et al.*, 2007; Sato *et al.*, 2011); *HAS2*, an essential enzyme to synthesize hyaluronan, which binds to ACAN producing stable accumulation of aggrecan around NP cells (Roughley *et al.*, 2011; Vigetti *et al.*, 2012) (Fig. 4, Table 1). Compared to HOsm/HP, *ACAN* and *CSGALNACT1* increased also under continuous HOsm/cyHP and continuous HOsm/coHP; however, *HAS2* was not upregulated. If sufficient hyaluronan is not produced, secreted aggrecan does not stably accumulate around each cell due to the lack of binding sites (Hascall and Heinegard, 1974). Immunohistological labelling using anti-KS revealed accumulation of KS around each NP cell and the absence of gaps in the ECM under repetitive HOsm/HP. Thus, repetition and switching between cyclic and constant HP played an anabolic role in forming NP ECM.

Col-2 was chosen as a typical phenotypic and anabolic marker of NP cells (Hayes *et al.*, 2001). The upregulation of *COL2A1* significantly increased with time under repetitive HOsm/HP, continuous HOsm/cyHP, and continuous HOsm/coHP compared to HOsm/No HP and LOsm/No HP conditions. Without HP, *COL2A1* expression remained steady under HOsm and declined under LOsm conditions over 18 d. Thus, osmolality in culture medium was probably a key condition to alter *COL2A1* expression. It is possible that this specificity of *COL2A1* upregulation was caused by a change in cell volume due to HOsm and changes to membrane channels [*e.g.*, TRPV4 (Johnson *et al.*, 2014)] since HP causes an increase in intracellular calcium concentration in chondrocytes (Mizuno, 2006). The effects of these physicochemical conditions, HOsm and HP, on *COL2A1* will be clarified during further study using potential inhibitors.

Catabolic/degenerative turnover

MMP13 expression was chosen as an enzymatic marker for the catabolism of collagen in NP cells (Le Maitre *et al.*, 2004). Application of HP in any mode significantly diminished *MMP13* expression, whereas it was significantly upregulated under LOsm/No HP conditions. Although the effects of deviatoric stress (Chan *et al.*, 2013) or interactions with other tissues were not examined, MMP13 was shown to be capable of destroying the ECM (Naqvi and Buckley, 2015; Yuan *et al.*, 2018) and stimulating angiogenesis. Therefore, HOsm and HP may have the potential to synergistically inhibit degeneration of NP tissue, including angiogenic invasion.

Col-1 is an essential component of the ECM; however, excess of Col-1 increases the risk of forming fibrotic tissue, causing dehydration of the NP tissue (Naqvi and Buckley, 2015; Yuan *et al.*, 2018). Thus, *COL1A1* expression was chosen as a marker of NP cell degeneration. Over 18 d culture, *COL1A1* expression was significantly upregulated in LOsm/No HP compared to other regimens, whereas HOsm (regardless of HP) could prevent fibrosis in NP and maintain hydration. However, applying HOsm conditions to body fluid is not a practical solution for regenerative therapy. To establish an HOsm-equivalent tissue environment, replenishing sulfated ECM to NP will be a practical alternative for restoring high ECM-associated OP.

Cellular characteristics

The upregulation of PCNA, a marker of proliferating NP cells (Johnson *et al.*, 2001), and ITGAV, an adhesion molecule mediating cell proliferation and stabilizing cell adhesion within the ECM (Gilchrist *et al.*, 2007; Le Maitre *et al.*, 2009; Nettles *et al.*, 2014), was significantly higher with HOsm/HP compared to other HP regimens by day 18. This suggested that proliferating cells produced the adhesion molecule integrin V, which binds to fibronectin in the ECM. The NP tissue is composed of abundant chondroitin sulfate, which prevents cell adhesion. For regenerative therapy, the presence of both collagen and fibronectin would be necessary to promote cell proliferation.

To evaluate changes in NP phenotypes, gene expression of *CDH2* (Hwang *et al.*, 2016; Risbud *et al.*, 2014) was measured. Under repetitive HOsm/HP, CDH2 expression was similar to that of other characteristic cellular molecules (PCNA, ITGV). Since CDH2 is a cell-cell contact molecule, proliferation of NP cells may efficiently occur within cell clusters, increasing to establish cell-cell contact. Although early studies showed that *CDH2* expression increases under cyHP and decreases under coHP (Wang *et al.*, 2017; Xu *et al.*, 2018), the present study results indicated that repetitive HOsm/HP elicited a significantly larger increase in *CDH2* compared to cyHP and coHP loading. The effects of repetitively alternating cyHP and coHP on *CDH2* expression will be clarified in further studies.

CTGF plays roles in both anabolic and catabolic turnover in NP cells. CTGF is a paracrine marker promoting fibrotic ECM production and leading to degeneration of NP tissue (Ali *et al.*, 2008; James *et al.*, 2019; Tran *et al.*, 2013). Under HOsm/No HP and H-LOsm/HP, *CTGF* showed a trend toward increased upregulation compared to other regimens over 18 d. However, these unique trends had large standard deviations of RQs. Even though further studies clarifying the effects of CTGF will be needed, other physicochemical stresses, *e.g.*, deviatoric stress, may affect CTGF due to more active fluid movement (Neidlinger-Wilke *et al.*, 2005).

Effects of repetitive regimen of H-LOsm/HP to recapitulate abnormal NP under diurnal spinal motion

A normal NP tissue contains sGAG, which are negatively charged and create an ECM-associated high OP. Axial compression and relaxation in the NP tissue, with the circadian rhythms of spinal motion, results in movement of intra-NP fluid as well as changes in the volume of the NP tissue within the IVD segment (Mavrogonatou and Kletsas, 2010). These changes in OP and HP were mimicked using an NP cell/cluster model. The effects of repetitive regimens of HOsm/cyHP (compressive NP with diurnal stress) followed by LOsm/coHP (bulging NP with no external stress but intradiscal HP) on metabolic turnover and cellular characteristics were examined.

Comparing HOsm/HP and H-LOsm/HP, the latter diminished the significant increase in gene expressions of most molecules or maintained lower levels over 18 d, except for *CTGF*. More specifically LOsm/No HP diminished the repetitive and cumulative effects of HP. To clarify the roles of HOsm and LOsm, the effects of the newly accumulated endogenous ECM need to be examined, which has the potential to create ECM-associated OP. LOsm after accumulation of ECM by NP cells instead of LOsm with no accumulation should be examined (Hoffmann *et al.*, 2009; Lodish *et al.*, 2000). Though H-LOsm/HP maintained most cellular characteristics, this regimen did not increase *COL2A1* and showed a trend toward increasing *CTGF*, indicating progressive degeneration. Once the IVD compartment is destroyed, it is very unlikely that metabolic turnover in NP cells can support regeneration on its own, clearing the way for biological therapeutic intervention.

Accumulation of sGAG and proliferation and viability of NP cells

sGAG and DNA of NP cells/clusters under HOsm/No HP and HOsm/HP were compared using pooled NP cells/clusters isolated from 5 tails (5 pouches at each time point) to avoid risk of batch-to-batch variation of NP cell isolation. Accumulation of sGAG under HOsm/No HP and HOsm/HP showed increasing trends and significant increase ($p < 0.01$) over 18 d, respectively. These increases should be consistent with upregulation of *ACAN* and *CSGALNACT1* (Fig.

4,7). However, there was no significant difference between HOsm/No HP and HOsm/HP conditions. A cumulative parameter of sGAG and a short-term parameter of gene expression should include correlations among multiple molecules. The amount of DNA under HOsm/No HP and HOsm/HP showed steady levels over 18 d of culture, whereas *PCNA* showed a slight increase under HOsm/HP compared to HOsm/No HP conditions. Since *COL1A1* showed low levels under both conditions over 18 d, NP cells had limited binding sites to ECM and, consequently, less DNA was measured. For promoting regeneration, cell adhesion on ECM and cell proliferation should be stimulated with other stress factors or augmented ECM materials.

Conclusions

The present study demonstrated that a repetitive regimen of HOsm/HP in NP cells increased gene expression and accumulation of ECM molecules, increased or maintained the proliferation capability and phenotypes of NP cells as well as suppressed the expression of degenerative/catabolic molecules over 18 d. Although bNP cells showed a higher anabolic turnover of *ACAN* and *COL2A1* under HOsm/HP, distinctive differences were found with *CSGALNACT1* and *HAS2* compared to continuous cyHP and continuous coHP. Thus, repetitive alternating cyHP and coHP could promote production of whole aggrecan components (core protein, chondroitin sulfate) and binding site (hyaluronan). The repetitive regimen also increased cell proliferation (*PCNA*), and cell-cell (*CDH2*) and cell-ECM (*ITGV*) adhesion molecules compared to other HP modes and no HP. Since cell proliferation is another important characteristic promoting regeneration of NP cells, repetitive regimens are necessary. Furthermore, HP with any mode and/or HOsm inhibited catabolic *MMP13* and minimized expression of its counterpart, fibril Col-1 (*COL1A1*) compared to LOsm/No HP. Balanced production and degradation of molecules is expected to proceed under repetitive regimens of HP.

Although amorphous NP tissue is under compressive stress, which consists of pure HP and pure deviatoric (distortional or shear) stress, the present study demonstrated only the effects of pure HP on production of ECM and the cellular behavior of NP cells. In future studies, the effects of compressive stresses, including deviatoric stress, should be examined. Additional stresses may reproduce upregulation of degenerative/catabolic turnover and cellular behavior. With a set of these stresses, it may be possible to model homeostasis or balance anabolic and catabolic turnover in NP cells by manipulating HP and deviatoric stress.

The present study tried to identify the effects of certain HPs and OPs on the biology of NP cells. A better understanding of how cells respond to physicochemical stresses will help treating the degenerating disc with either cell- or gene-based therapies and other potential matrix-enhancing therapies. Efforts to apply these tissue-engineering and regenerative-medicine strategies will need to consider these important physicochemical stresses that may have a major impact on the survivability of such treatments.

Acknowledgements

F.A.V. was awarded a scholarship from the CAPES Foundation, Programa de Doutorado Sanduiche no Exterior, Brazil (Finance code 001). We thank Paul Guttry for assistance in manuscript preparation.

References

Alentado VJ, Lubelski D, Healy AT, Orr RD, Steinmetz MP, Benzel EC (2016) Predisposing characteristics of adjacent segment disease after lumbar fusion. Spine (Phila Pa 1976) **41**: 1167-1172.

Ali R, Le Maitre CL, Richardson SM, Hoyland JA, Freemont AJ (2008) Connective tissue growth factor expression in human intervertebral disc: implications for angiogenesis in intervertebral disc degeneration. Biotech Histochem **83**: 239-245.

Alini M, Eisenstein SM, Ito K, Little C, Kettler AA, Masuda K, Melrose J, Ralphs J, Stokes I, Wilke HJ (2008) Are animal models useful for studying human disc disorders/degeneration? Eur Spine J **17**: 2-19.

Alvin MD, Qureshi S, Klineberg E (2014) Cervical degenerative disease: systematic review of economic analyses. Spine (Phila Pa 1976) **39**: S53-64.

Ayotte DC, Ito K, Tepic S (2001) Direction-dependent resistance to flow in the endplate of the intervertebral disc: an *ex vivo* study. J Orthop Res **19**: 1073-1077.

Carter DR, Beaupre GS (2001) In: Skeletal function and form. Cambridge University Press, New York, NY, USA.

Chan SCW, Ferguson SJ, Gantenbein-Ritter B (2011) The effects of dynamic loading on the intervertebral disc. Eur Spine J **20**: 1796-1812.

Chan SCW, Walser J, Kappeli P, Shamsollahi MJ, Ferguson SJ, Gantenbein-Ritter B (2013) Region specific response of intervertebral disc cells to complex dynamic loading: an organ culture study using a dynamic torsion-compression bioreactor. PLoS One **8**: e72489. DOI: 10.1371/journal.pone.0072489.

Demers CN, Antoniou J, Mwale F (2004) Value and limitations of using the bovine tail as a model for the human lumbar spine. Spine (Phila Pa 1976) **29**: 2793-2799.

Detiger SEL, Bakker JY, Emanuel KS, Schmitz M, Vergroesen PPA, van der Veen AJ, Mazel C, Smit TH (2016) Translational challenges for the development of a novel nucleus pulposus substitute: experimental

results from biomechanical and *in vivo* studies. J Biomater Appl **30**: 983-994.

Emanuel KS, Vergroesen P-PA, Peeters M, Holewijn RM, Kingma I, Smit TH (2015) Poroelastic behaviour of the degenerating human intervertebral disc: a ten-day study in a loaded disc culture system. Eur Cell Mater **29**: 330-340.

Farndale RW, Sayers CA, Barrett AJ (1982) A direct spectrophotometric microassay for sulfated glycosaminoglycan in cartilage cultures. Connect Tissue Res **9**: 247-248.

Gantenbein B, Grunhagen T, Lee CR, van Donkelaar CC, Alini M, Ito K (2006) An *in vitro* organ culturing system for intervertebral disc explants with vertebral endplates: a feasibility study with ovine caudal discs. Spine (Phila Pa 1976) **31**: 2665-2673.

Gilchrist CL, Chen J, Richardson WJ, Loeser RF, Setton LA (2007) Functional integrin subunits regulating cell-matrix interactions in the intervertebral disc. J Orthop Res **25**: 829-840.

Handa T, Ishihara H, Ohshima H, Osada R, Tsuji H, Obata K (1997) Effects of hydrostatic pressure on matrix synthesis and matrix metalloproteinase production in the human lumbar intervertebral disc. Spine (Phila Pa 1976) **22**: 1085-1091.

Hascall VC, Heinegard D (1974) Aggregation of cartilage proteoglycan: oligosaccharide competitors of the proteoglycan-hyaluronic acid interaction. J Biol Chem **249**: 4242-4249.

Haschtmann D, Stoyanov JV, Ferguson SJ (2006) Influence of diurnal hyperosmotic loading on the metabolism and matrix gene expression of a whole-organ intervertebral disc model. J Orthop Res **24**: 1957-1966.

Hayes AJ, Benjamin M, Ralphs JR (2001) Extracellular matrix in development of the intervertebral disc. Matrix Biol **20**: 107-121.

Hoffmann EK, Lambert IH, Pedersen SF (2009) Physiology of cell volume regulation in vertebrates. Physiol Rev **89**: 193-277.

Hutton WC, Elmer WA, Boden SD, Hyon S, Toribatake Y, Tomita K, Hair GA (1999) The effect of hydrostatic pressure on intervertebral disc metabolism. Spine (Phila Pa 1976) **24**: 1507-1515.

Hutton WC, Elmer WA, Bryce LM, Kozlowska EE, Boden SD, Kozlowski M (2001) Do the intervertebral disc cells respond to different levels of hydrostatic pressure? Clin Biomech **16**: 728-734.

Hwang PY, Jing L, Chen J, Lim FL, Tang R, Choi H, Cheung KM, Risbud MV, Gersbach CA, Guilak F, Leung VY, Setton LA (2016) N-cadherin is key to expression of the nucleus pulposus cell phenotype under selective substrate culture conditions. Sci Rep **6**: 28038. DOI: 10.1038/srep28038.

Ishihara H, Warensjo K, Roberts S, Urban J (1997) Proteoglycan synthesis in the intervertebral disk nucleus: the role of extracellular osmolality. Am J Physiol **272**: C1499-1506.

Ishimaru D, Sugiura N, Akiyama H, Watanabe H, Matsumoto K (2014) Alternations in the chondroitin sulfate chain in human osteoarthritic cartilage of the knee. Osteoarthritis Cartilage **22**: 250-258.

James G, Klyne DM, Millecamps M, Stone LS, Hodges PW (2019) Physical activity attenuates fibrotic alterations to the multifidus muscle associated with intervertebral disc degeneration. Eur Spine J **28**: 893-904.

Johnson WE, Eisenstein SM, Roberts S (2001) Cell cluster formation in degenerate lumber intervertebral discs is associated with increased disc cell proliferation. Connect Tissue Res **42**: 197-207.

Johnson ZI, Shapiro IM, Risbud MV (2014) Extracellular osmolarity regulates matrix homeostasis in the intervertebral disc and articular cartilage: evolving role of TonEBP. Matrix Biol **40**: 10-16.

Kasra M, Merryman WD, Loveless KN, Goel VK, Martin JD, Buckwalter JA (2006) Frequency response of pig intervertebral disc cells subjected to dynamic hydrostatic pressure. J Orthop Res **24**: 1967-1973.

Kim Y, Sah RL, Doong JY, Grodzinsky AJ (1988) Fluorometric assay of DNA in cartilage explant using Hoechst 33258. Anal Biochem **174**: 168-176.

Le Maitre CL, Freemont AJ, Hoyland JA (2004) Localization of degradative enzymes and their inhibitors in the degeneration human intervertebral disc. J Pathol **204**: 47-54.

Le Maitre CL, Frain J, Fotheringham AP, Freemont AJ, Hoyland JA (2008) Human cells derived from degenerate intervertebral discs respond differently to those derived from non-degenerate intervertebral discs following application of dynamic hydrostatic pressure. Biorheology **45**: 563-575.

Le Maitre CL, Frain J, Millward-Sadler J, Fotheringham AP, Freemont AJ, Hoyland JA (2009) Altered integrin mechnotrasnduction in human nucleus pulposus cells derived from degenerated discs. Arthritis Rheum **60**: 460-469.

Le Maitre CL, Fotheringham AP, Freemont AJ, Hoyland JA (2009) Development of an *in vitro* model to test the efficacy of novel therapies for IVD degeneration. J Tissue Eng Regen Med **3**: 461-469.

Lodish H, Berk A, Zipursky SL, Matsudaira P, Baltimore D, Darnell J (2000) Osmosis, water channels, and the regulation of cell volume. In: Molecular Cell Biology. 4th edition, WH Freeman and Company, New York, NY, USA.

Makhni MC, Caldwell JE, Saifi C, Fischer CR, Lehman RA, Lenke LG, Lee FY (2016) Tissue engineering advances in spine surgery. Regen Med **11**: 211-222.

Mavrogonatou E, Kletsas D (2010) Effect of varying osmotic conditions on the response of bovine nucleus pulposus cells to growth factors and the activation of the ERK and Akt pathway. J Orthop Res **28**: 1276-1282.

Mizuno S, Ogawa R (2011) Using changes in hydrostatic and osmotic pressure to manipulate metabolic function in chondrocytes. Am J Physiol Cell Physiol **300**: C1234-1245.

Mizuno S, Kashiwa K, Kang JD (2019) Molecular and histological characteristics of bovine caudal

nucleus pulposus by combined changes in hydrostatic and osmotic pressures *in vitro*. J Orthop Res **37**: 466-476.

Naqvi SM, Buckley CT (2015) Extracellular matrix production by nucleus pulposus and bone marrow stem cells in response to altered oxygen and glucose microenvironments. J Anat **227**: 757-766.

Neidlinger-Wilke C, Mietsch A, Rinkler C, Wilke H-J, Ignatius A, Urban JPG (2012) Interactions of environmental conditions and mechanical loads influence on matrix turnover by nucleus pulposus cells. J Orthop Res **30**: 112-121.

Neidlinger-Wilke C, Galbusera F, Pratsinis H, Mavrogonatou E, Mietsch A, Kletsas D, Wilke H (2014) Mechanical loading of the intervertebral disc: from the macroscopic to the cellular level. Eur Spine J **23**: S333-343.

Neidlinger-Wilke C, Würtz K, Liedert A, Schmidt C, Börm W, Ignatius A, Wilke H-J, Claes L. (2005) A three-dimensional collagen matrix as a suitable culture system for the comparison of cyclic strain and hydrostatic pressure effects on intervertebral disc cells. J Nurosurg: Spine **2**: 457-465.

Nettles DL, Richardson WJ, Setton LA (2014) Integrin expression in cells of the intervertebral disc. J Anat **204**: 515-520.

Ogura T, Tsuchiya A, Minas T, Mizuno S (2019) Engineering a human articular chondrocyte construct manipulated by hydrostatic pressure and deviatoric stress. J Tissue Eng Regen Med **13**: 1143-1152.

Oshima H, Ishihara H, Urban JPG, Tsuji H (1993) The use of coccygeal disks to study intervertebral disc metabolism. J Orthop Res **11**: 332-338.

Papadopoulos NG, Dedoussis GV, Spanakos G, Gritzapis AD, Baxevanis CN, Papamichail M (1994) An improved fluoresce assay for the determination of lymphocyte-mediated cytotoxity using flow cytometry. J Immunol Methods **177**: 101-111.

Risbud MV, Shapiro IM (2014) Role of cytokines in intervertebral disc degeneration: pain and disc content. Nat Rev Rheumatol **10**: 44-56.

Rosenzweig DH, Fairag R, Mathieu AP, Li L, Eglin D, Este MD, Steffen T, Weber MH, Ouellet JA, Haglund L (2018) Thermoreversible hyaluronan-hydrogel and autologous nucleus pulposus cell delivery regenerates human intervertebral discs and *ex vivo*, physiological organ culture model. Eur Cell Mat **36**: 200-217.

Roughley PJ, Lamplugh L, Lee ER, Matsumoto K, Yamaguchi Y (2011) The role of hyaluronan produced by Has2 gene expression in development of the spine. Spine (Phila Pa 1976) **36**: E914-E920.

Sakai D, Schol J (2017) Cell therapy for intervertebral disc repair: clinical perspective. J Orthop Translat **9**: 8-18.

Sakai K, Kimata K, Sato T, Gotoh M, Narimatsu H, Shinomiya K, Watanabe H (2007) Chondroitin sulfate N-Acetylgalactosaminyltransferase-1 plays a critical role in chondroitin sulfate synthesis in cartilage. J Biol Chem **282**: 4152-4161.

Sato K, Kikuchi S, Yonezawa T (1999) *In vivo* intradscal pressure measurement in healthy individuals and in patients with ongoing back problems. Spine (Phila Pa 1976) **24**: 2468-2474.

Sato T, Ikehara Y, Ogawa H, Hirano T, Kiyohara K, Hagiwara K, Togayachi A, Ema M, Takahashi S, Kimata K, Watanabe H, Narimatsu H (2011) Chondroitin sulfate N-acetylgalactosaminyltransferase 1 is necessary for normal endochondral ossification and aggrecan metabolism. J Biol Chem **286**: 5803-5812.

Senteler M, Weisse B, Rothenfluh DA, Farshad MT, Snedeker JG (2017) Fusion angle affects intervertebral adjacent spinal segment joint forces-model-based analysis of patient specific alignment. J Orthop Res **35**: 131-139.

Shah BS, Chahine NO (2018) Dynamic hydrostatic pressure regulates nucleus pulposus phenotypic expression and metabolism in a cell density-dependent manner. J Biomech Eng **140**: 021003. DOI: 10.1115/1.4038758.

Smith LJ, Silverman L, Sakai D, Le Maitre CL, Mauck RL, Malhotra NR, Lotz JC, Buckley CT (2018) Advancing cell therapies for intervertebral disc regeneration from the lab to the clinic: recommendation of the ORS spine section. JOR Spine **1**: e1036. DOI: 10.1002/jsp2.1036.

Snider RK, Krumwiede NK, Snider LJ, Jurist JM, Lew RA, Katz JN (1999) Factors affecting lumbar spinal fusion. J Spinal Disord **12**: 107-114.

Takeoka Y, Kang JD, Mizuno S (2020) *In vitro* nucleus pulposus tissue model with physicochemical stresses. JOR Spine **3**: e1105. DOI: 10.1002/jsp2.1105.

Thorpe PP, Li Y, Yao L (2016) Advances in biological therapy for nucleus pulposus regeneration. Osteoarthritis Cartilage **24**: 206-212.

Tran CM, Shapiro IM, Risbud MV (2013) Molecular regulation of CCN2 in the intervertebral disc: lessons learned from other connective tissues. Matrix Biol **32**: 298-306.

Tyrrell AR, Reilly T, Troup JDG (1985) Circadian variation in stature and the effects of spinal loading. Spine (Phila Pa 1976) **10**: 161-164.

Urban JPG, McMullin JF (1988) Swelling pressure of the lumbar intervertebral discs: influence of age, spinal level, composition, and degeneration. Spine (Phila Pa 1976) **13**: 179-187.

Vergroesen PP, van der Veen AJ, van Royen BJ, Kingma I, Smit TH (2014) Intradiscal pressure depends on recent loading and correlates with disc height and compressive stiffness. Eur Spine J **23**: 2359-2368.

Vergroesen PP, van der Veen AJ, Emanuel KS (2016) The poroelastic behaviour of the intervertebral disc: a new perspective on diurnal fluid flow. J Biomech **49**: 857-863.

Vigetti D, Deleonibus S, Moretto P, Karousou E, Viola M, Bartolini B, Hascall VC, Tammi M, De Luca G, Passi A (2012) Role of UDP-N-acetylglucosamine (GlcNAc) and O-GlcNAcylation of hyaluronan synthase 2 in the control of chondroitin sulfate and hyaluronan synthesis. J Biol Chem **287**: 35544-35555.

Walter BA, Korecki CL, Purmessur D, Roughley PJ. Michalek AJ, Iatridis JC (2011) Complex loading affects intervertebral disc mechanics and biology. Osteoarthritis Cartilage **19**: 1011-1018.

Wang Z, Leng J, Zhao Y, Yu D, Xu F, Song Q, Qu Z, Zhuang X, Liu Y (2017) N-Cadherin maintains the healthy biology of nucleus pulposus cells under high-magnitude compression. Cell Physiol Biochem **43**: 2327-2337.

Wilke HJ, Neef P, Caimi M (1999) New *in vivo* measurement of pressures in the intervertebral disc in daily life. Spine (Phila Pa 1976) **24**: 755-762.

Wuertz K, Urban JP, Klasen J (2007) Influence of extracellular osmolarity and mechanical stimulation on gene expression of intervertebral disc cells. J Orthop Res **25**: 1513-1522.

Xu Y, Yao H, Li P, Xu W, Zhang J, Lv L, Teng H, Guo Z, Zhao H, Hou G (2018) Dynamic compression promotes the matrix synthesis of nucleus pulposus cells through up-regulating N-CDH expression in a perfusion bioreactor culture. Cell Physiol Biochem **46**: 482-491.

Yuan M, Pai PJ, Liu X, Lam H, Chan BP (2018) Proteomic analysis of nucleus pulposus cell-derived extracellular matrix niche and its effect on phenotypic alteration of dermal fibroblasts. Sci Rep **8**: 1512. DOI: 10.1038/s41598-018-19931-9.

Zvicer J, Obradovic B (2018) Bioreactors with hydrostatic pressures imitating physiological environment in intervertebral discs. J Tissue Eng Regen Med **12**: 529-545.

Discussion with Reviewers

Reviewer: HP has also been shown to have beneficial effects on the phenotype of articular chondrocytes. Are there any differences in the optimal loading regimes between IVD and cartilage cells?
Authors: We have previously demonstrated that cyHP 0-0.5 MPa, 0.5 Hz stimulates the upregulation of cartilaginous matrix genes in bovine articular chondrocytes (Mizuno *et al.*, 2011). The same was proven for bNP cells/clusters (Mizuno *et al.*, 2019). However, ECM accumulated by NP cells showed gaps (spatial voids) when 7 μm-thick sections were labelled with anti-KS antibody, whereas ECM formed by articular chondrocytes did not show gaps. Based on this histological difference, we hypothesized that coHP prevented formation of gaps because the NP is under intradiscal pressure. HOsm/cyHP at 0.2-0.7 MPa for 2 d followed by HOsm/coHP at 0.3 MPa for 1 d upregulates cartilaginous matrix molecules and reduces gap formation (Takeoka *et al.*, 2020). In the present study, this regimen of HOsm/HP was repeated over 18 d and synthesis and accumulation of cartilaginous molecules was shown using gene expression, immunohistological, and biochemical markers. When we design any experiments to determine differences between more than two treatment groups, we are careful to choose advantageous markers and treatments. Thus, although our findings should be interpreted with the normal limitations of any *in vitro* experiment, the data should be suitable for extrapolation of the effects of HP *in vivo*. As we gather more information on varied culture conditions, we will establish an IVD model for developing regenerative therapeutic strategies.

Joana R Ferreira: How would you adjust the protocol to induce a degenerative state that closely mimics the gradual IVD degeneration that occurs with aging?
Authors: The present study elucidated the effects of pure HP on NP cells/clusters. Native NP is under compressive stresses, which include pure HP and deviatoric stress (distortional stress). The present study did not consider aging cells and degenerated ECM (altered balance of ECM components). The pathophysiological mechanism of the aging process is not considered the same process as disc degeneration. Certainly, there are overlapping molecular mechanisms but clearly distinct patterns. For instance, the aging mechanism involves DNA damage and low-grade inflammation whereas pathological degeneration involves biomechanical mechanisms as well as low-grade inflammation.

Certainly, in the described *in vitro* model, it was possible to mimic low-grade inflammation by applying inflammatory cytokines such as interleukin-1 or tumor necrosis factor alpha, as many other groups have done. Perhaps we will consider doing these experiments in the future to better understand the molecular mechanisms of how osmotic and hydrostatic pressures can potentially mitigate such degenerative pathways.

Joana R Ferreira: How would you envision the complexation of this model to include the influence of annulus fibrosus cells to the anabolic/catabolic response of the IVD, under the biomechanical stimuli studied?
Authors: We focused on the effects of HP in cellular and metabolic turnover in bNP cells under a defined algorithm of repetitive cyclic and constant HP. Obviously, NP tissue is exposed to compressive loading, which includes HP and deviatoric/distortional stresses. The annulus fibrosus tissue has different architectural composition and is predominantly composed of collagen fibers as well as other matrix proteins; therefore, it may not be governed by OP as much as NP cells, which are in a different matrix environment. Nevertheless, the cells of the annulus fibrosis with no doubt react to mechanical loading, such as the deviatoric stress, and may even respond to various OPs that occur within the nucleus pulposus. There is no doubt some degree of crosstalk between the NP and the annulus fibrosus, making this an area of future study.

Joana R Ferreira: How do you imagine these findings can be used to design a therapeutic approach capable of promoting a healthy anabolic turnover of the NP?

Authors: This report intended to emphasize how cellular and metabolic turnover proceed under repetitive physical chemical stress. As mention above, deviatoric stress, which may contribute to the degenerative cascade, still need to be incorporated. The present study tried to identify the effects of HP and OP on the biology of NP cells. With a better understanding of how cells respond to these types of physicochemical stresses, we will be much better armed when biologically treating the degenerating disc with either cell- or gene-based therapies and other potential matrix-enhancing therapies. Many investigators are looking for basic biological enhancements for therapy without considering these important physicochemical stresses that may have major impact on the survivability of such treatments.

Editor's note: The Scientific Editor responsible for this paper was Sibylle Grad.